

UC Davis

UC Davis Previously Published Works

Title

Canine epidermal neural crest stem cells: characterization and potential as therapy candidate for a large animal model of spinal cord injury.

Permalink

<https://escholarship.org/uc/item/9g1323f9>

Journal

Stem cells translational medicine, 3(3)

ISSN

2157-6564

Authors

Gericota, Barbara
Anderson, Joseph S
Mitchell, Gaela
et al.

Publication Date

2014-03-01

DOI

10.5966/sctm.2013-0129

Peer reviewed



Canine Epidermal Neural Crest Stem Cells: Characterization and Potential as Therapy Candidate for a Large Animal Model of Spinal Cord Injury

BARBARA GERICOTA,^a JOSEPH S. ANDERSON,^a GAELA MITCHELL,^a DORI L. BORJESSON,^b
BEVERLY K. STURGES,^c JAN A. NOLTA,^a MAYA SIEBER-BLUM^d

Key Words. Neural crest • Adult stem cells • EPI-NCSC • Canine epidermal neural crest stem cells • cEPI-NCSC • Dog model • Spinal cord injury • Hair follicle

ABSTRACT

The discovery of multipotent neural crest-derived stem cells, named epidermal neural crest stem cells (EPI-NCSC), that persist postnatally in an easy-to-access location—the bulge of hair follicles—opens a spectrum of novel opportunities for patient-specific therapies. We present a detailed characterization of canine EPI-NCSC (cEPI-NCSC) from multiple dog breeds and protocols for their isolation and ex vivo expansion. Furthermore, we provide novel tools for research in canines, which currently are still scarce. In analogy to human and mouse EPI-NCSC, the neural crest origin of cEPI-NCSC is shown by their expression of the neural crest stem cell molecular signature and other neural crest-characteristic genes. Similar to human EPI-NCSC, cEPI-NCSC also expressed pluripotency genes. We demonstrated that cEPI-NCSC can generate all major neural crest derivatives. In vitro clonal analyses established multipotency and self-renewal ability of cEPI-NCSC, establishing cEPI-NCSC as multipotent somatic stem cells. A critical analysis of the literature on canine spinal cord injury (SCI) showed the need for novel treatments and suggested that cEPI-NCSC represent viable candidates for cell-based therapies in dog SCI, particularly for chondrodystrophic dogs. This notion is supported by the close ontological relationship between neural crest stem cells and spinal cord stem cells. Thus, cEPI-NCSC promise to offer not only a potential treatment for canines but also an attractive and realistic large animal model for human SCI. Taken together, we provide the groundwork for the development of a novel cell-based therapy for a condition with extremely poor prognosis and no available effective treatment. *STEM CELLS TRANSLATIONAL MEDICINE* 2014;3:334–345

INTRODUCTION

There were two goals for the present study: to determine whether the canine hair follicle contains epidermal neural crest stem cells (EPI-NCSC) and to design and create novel canine-specific tools for the visualization and analysis of canine stem cells. The discovery of multipotent neural crest stem cells (NCSC) that persist postnatally into adulthood in an easily accessible location, the bulge of hair follicles, opens a spectrum of opportunities for cell-based therapies. As neural crest derivatives, these stem cells have a high degree of innate developmental plasticity. EPI-NCSC can be accessed with ease from haired skin biopsies. By taking advantage of the migratory ability of neural crest cells, EPI-NCSC can be isolated as highly pure populations of multipotent stem cells, and they can be expanded ex vivo into millions of stem cells within a short period of time [1, 2].

The neural crest is a transient embryonic structure in vertebrates that originates in the neural folds. Neural crest cells migrate from the dorsal aspect of the forming neural tube via distinct

pathways to specific locations in the embryo, where they give rise to a wide array of cell types and tissues in the adult vertebrate organism [3–6]. Neural crest derivatives include the autonomic and enteric nervous systems, most primary sensory ganglia, craniofacial mesenchyme, endocrine cells such as the adrenal medulla, and smooth musculature of the cardiac outflow tract and the great vessels, among others [4, 7]. Neural crest cells also invade the ectoderm [8] and come to reside in the bulge of hair follicles [1, 2], a stem cell niche adjacent to the epidermal outer root sheath of hair follicles, where they form a reservoir of multipotent stem cells predestined to become pigment cell precursors, which in turn differentiate into melanocytes and give hair its color.

The strategy for establishing the neural crest origin of canine EPI-NCSC was based on our previous studies. EPI-NCSC were discovered in the mouse [1, 2]. Their neural crest origin was determined unequivocally by using cells from the *Wnt1-cre:R26R* compound transgenic mouse in which neural crest cells and their progeny are indelibly and specifically marked by their expression

^aStem Cell Program, Institute for Regenerative Cures Sacramento, California, USA;

^bDepartment of Pathology, Microbiology and Immunology and

^cDepartment of Surgical and Radiological Sciences, School of Veterinary Medicine, University of California, Davis, Davis, California, USA;

^dInstitute of Genetic Medicine, Centre for Life, Newcastle University, Newcastle upon Tyne, United Kingdom

Correspondence: Maya Sieber-Blum, Ph.D., Institute of Genetic Medicine, Centre for Life, Newcastle University, Newcastle upon Tyne, NE1 3BZ, United Kingdom. Telephone: 44-191-241-8638; E-Mail: maya.sieber-blum@ncl.ac.uk

Received July 18, 2013; accepted for publication October 23, 2013; first published online in *SCTM EXPRESS* January 17, 2014.

©AlphaMed Press
1066-5099/2014/\$20.00/0

<http://dx.doi.org/10.5966/sctm.2013-0129>

of β -galactosidase [1, 2]. We performed gene expression profiling of mouse embryonic NCSC and mouse EPI-NCSC [9]. By in silico comparisons, we defined an NCSC molecular signature, which is specific to both embryonic and adult NCSC. By comparing the neural crest molecular signature with published gene expression profiles, we determined that mouse EPI-NCSC were distinctly different from any other known skin-resident stem cells or progenitors [9, 10]. By analogy, we subsequently characterized human EPI-NCSC (hEPI-NCSC) and found that hEPI-NCSC also express the NCSC molecular signature, as well as other established NCSC markers [11]. The goal in the current study was to determine whether dog hair follicles contain migratory cells that express the NCSC molecular signature and other pertinent NCSC genes. We show that such stem cells indeed exist in various dog breeds.

Neural crest cells are ontologically closely related to spinal cord stem cells because they share a higher order stem cell that gives rise to both neural tube stem cells and NCSC [12]. For this reason, EPI-NCSC are attractive candidates for cell-based therapies in models of spinal cord injury (SCI). In fact, in mouse models of SCI, mouse EPI-NCSC exhibited several advantageous characteristics, including cell replacement, neuroprotection, angiogenesis, and modulation of scar formation, which together led to an approximately 20% improvement in sensory connectivity and touch perception [13–15].

In human and veterinary medicine, SCI is a serious neurological problem with severe and permanent debilitating neurological deficits. The irreversible loss of function consequent to loss of spinal cord parenchyma has long been recognized, and despite intense effort, successful therapies are still not available [16, 17]. Recent advances in the understanding of the pathophysiology of SCI have produced many chemical, cellular, and physical interventions that appear promising in vitro or in laboratory animal models [18–21]; however, translation into effective treatment for human or animal patients has not yet been achieved. This “translation gap” results in part from the lack of testing in realistic models for spontaneous SCI [22–25]. Spontaneous SCI is a common neurological problem in dogs, with marked similarities, clinically and pathologically, to the syndrome in people [22, 23, 25, 26]. For this reason, dogs provide a readily accessible, clinically relevant, spontaneously arising model for evaluation of EPI-NCSC therapeutic intervention. In this study, we provide the groundwork for future research toward the development of a potentially novel therapy for a condition with extremely poor prognosis and no available effective treatment.

MATERIALS AND METHODS

Bulge Explants and Isolation of cEPI-NCSC

All tissues from haired skin on the dorsum and leg were obtained from surgical biopsy or necropsy samples, after owner authorization for use of canine patients presented at the Veterinary Medical Teaching Hospital at University of California Davis, with ethical approval by the University of California Davis Institutional Animal Care and Use Committee, protocol number 16649. Canine hair follicles were microdissected, as we have described previously [1, 2, 9]. Attention was paid to the compound nature of the canine follicular anatomy [27]. Primary and secondary hair follicles in anagen phase were identified and dissected separately. The midfollicular area was excised and cut in half, and each piece was placed into a CellStart-coated (Invitrogen, Paisley, U.K., <http://www.invitrogen.com>; catalog no. A10142-01) well of 24-well plates.

Hair follicular explants adhered to the substratum within 1 hour. The explants were incubated in a humidified atmosphere at 37°C, 5% CO₂, 5% O₂. The culture medium consisted of NeuroCult XF (Stem-Cell Technologies, Grenoble, France, <http://www.stemcell.com>; catalog no. 05761) supplemented with 10 ng/ml rhFGF2 (R&D Systems, Abingdon, U.K., <http://www.rndsystems.com>; catalog no. 233-FB), 20 ng/ml rhEGF (R&D Systems; catalog no. 236-EG), 1× insulin-transferrin-selenium (Invitrogen; catalog no. 41400-045), 1× linoleic acid-oleic acid-albumin (Sigma-Aldrich, Poole, U.K., <http://www.sigmaaldrich.com>; catalog no. L9655), 5% fetal bovine serum (FBS; HyClone; Thermo Fisher, Cramlington, U.K., <http://www.thermofisher.com>; catalog no. SH30070.02), 1× GlutaMAX (Invitrogen; catalog no. 35050), 1× penicillin/streptomycin (Sigma-Aldrich; catalog no. P0781), and amphotericin B (Sigma-Aldrich; catalog no. A2942).

At 4–7 days following onset of emigration of cEPI-NCSC from the bulge explant, follicular explants were removed with a bent, electrolytically sharpened tungsten needle. For subculture, cells were rinsed with Dulbecco’s phosphate-buffered saline (PBS; Invitrogen; catalog no. 14190) and detached by incubation with 1× TrypLE Select (Invitrogen; catalog no. 12563) for 2 minutes. Treatment was stopped by adding culture medium, and the virtually single-cell cell suspension was collected. The cells were seeded at 2,500 cells per 35-mm CellStart-coated culture plate and expanded in the same culture medium. At the end of the expansion period (5–7 days), cells were either dissolved in TRIzol (Invitrogen; catalog no. 15596-018) for RNA isolation or isolated with TrypLE (Invitrogen; catalog no. 12563), as described previously, and either used for clonal analysis or seeded onto glass coverslips for indirect immunocytochemistry, as described below.

Dog-Specific Primer Design and Testing

Fresh tissue was snap frozen and stored at –80°C until RNA extraction. Samples from brain, 21-day-old embryo, placenta, testis, uterus, ovary, and colon were obtained from biopsy or necropsy tissues from five different dogs. cEPI-NCSC were isolated from hair follicles, as described previously. For reverse transcription, total RNA was extracted with TRIzol reagent and treated with DNase I (New England BioLabs, Ipswich, MA, <http://www.neb.com>; catalog no. M0303S). TaqMan reverse transcription reagents (Applied Biosystems, Foster City, CA, <http://www.appliedbiosystems.com>; catalog no. N808-0234) were used for reverse transcription, following the manufacturer’s instructions.

A panel of 11 genes that included NCSC molecular signature genes, other neural crest markers, and a general stem cell marker were selected based on our previous work: *msh* homeobox 2 (*Msx2*), thimet oligopeptidase 1 (*Thop1*), myosin X (*Myo10*), *vets* erythroblastosis virus E26 oncogene homolog 1 (avian) (*Ets1*), ADAM metalloproteinase domain 12 (*Adam12*), collapsin response mediator protein 1 (*Crmp1*), ubiquitination factor E4B (*Ube4b*), crystallin α B (*Cryab*), SRY (sex determining region Y)-box 10 (*Sox10*), snail homolog 2 (*Snai2*), and nestin (*Nes*) [9, 11].

The pluripotency markers selected were based on previous work. Sequences were obtained from the GenBank database (National Center for Biotechnology Information [NCBI], Bethesda, MD, <http://www.ncbi.nlm.nih.gov/genbank/>): POU class 5 homeobox 1 (*POU5F1*, also known as *Oct4*), SRY (sex determining region Y)-box 2 (*Sox2*), Krüppel-like factor 4 (*Klf4*), *c-myc* proto-oncogene (*c-Myc*), and lin-28 homolog A (*Caenorhabditis elegans*) (*Lin28a*, also known as *Lin28*).

Housekeeping genes were selected from a detailed study that developed and evaluated canine reference genes for accurate quantification of gene expression [28]. The following three housekeeping genes were used: β -2-microglobulin (B2M), ribosomal protein S5 (RPS5), and ribosomal protein S19 (RPS19).

Primer sets were developed using known dog sequences available from GenBank (supplemental online Table 1). Primers were designed using the OligoPerfect Designer software (Life Technologies, Rockville, MD, <http://www.lifetech.com>). Uniqueness and specificity of each primer were verified using a Basic Local Alignment Search Tool (NCBI, <http://blast.ncbi.nlm.nih.gov/Blast.cgi>). Reverse transcriptase polymerase chain reaction (RT-PCR) was performed for the primer testing using USB FidelityTaq PCR Master Mix (Affymetrix, Santa Clara, CA, <http://www.affymetrix.com>; catalog no. 71182). Amplification was performed on a BioRad C1000 thermocycler under the following conditions: 94°C (3 minutes) followed by 40 cycles at 94°C (30 seconds), 60°C (30 seconds), and 72°C (30 seconds). For all primer sets, a non-reverse-transcribed RNA template was used as a negative control for genomic DNA contamination, water was used as a negative control, and embryo cDNA was used as a positive control.

RT-PCR products were cloned and sequenced to confirm their identity. Briefly, according to the manufacturer's instructions, DNA from RT-PCR products was gel extracted (Qiagen, Hilden, Germany, <http://www.qiagen.com>; catalog no. 28704) and cloned into the TOPO vector (Life Technologies; catalog no. K4500-01SC), and the reaction was transformed into competent bacteria (Life Technologies; catalog no. K4500-01SC). Amplified plasmid DNA was purified using a miniprep kit (Qiagen; catalog no. 27405). Subsequently, the DNA was digested with EcoRI enzyme (New England Biolabs; catalog no. R0101S), and selected samples were sequenced (Laragen, Culver City, CA, <http://www.laragen.com/>).

Real-Time Quantitative RT-PCR

Reverse transcription was done as described in the dog-specific primer design and testing section. Real-time quantitative RT-PCR (qPCR) was based on the high-affinity, double-stranded DNA-binding dye SYBR Green using Power SYBR Green PCR Master Mix (Applied Biosystems; catalog no. 4367659). Dog-specific primer sets were used (supplemental online Table 1). Reactions were done in triplicate. Amplification conditions were as follows: 95°C (10 minutes) followed by 40 cycles at 95°C (15 seconds) and 60°C (60 seconds), with one final cycle at 95°C (15 seconds), 60°C (60 seconds), and 95°C (15 seconds). Amplifications were performed in an Applied Biosystems 7300 Real Time PCR System thermocycler. A single amplification peak was observed on dissociation curve analysis of each reaction. Ct values for targets were normalized to the average Ct values of three housekeeping genes and expressed as the percentage thereof. For all markers tested, a non-reverse-transcribed RNA template was used as a negative control for genomic DNA contamination, and water was used as a negative control.

Indirect Immunofluorescence

Briefly, cell cultures were fixed in ice-cold 4% (wt/vol) paraformaldehyde in PBS (Invitrogen; catalog no. 20012) at room temperature for 30 minutes, followed by three 20-minute PBS washes, blocked with 2% (vol/vol) normal goat serum (Sigma-Aldrich; catalog no. G9023) in PBS at room temperature for 20 minutes. Primary antibody previously diluted in PBS, 0.1% (vol/vol) Triton X-100

was incubated overnight at 4°C. Subsequently, cultures were washed four times with PBS for 20 minutes each, followed by the addition of secondary antibody diluted 1:200 in PBS and incubated in the dark for 2 hours at room temperature. After removal of secondary antibody, cultures were washed four times with PBS for 20 minutes each. Finally, samples were mounted with Vectashield plus 4',6-diamidino-2-phenylindole (DAPI; Vector Laboratories, Peterborough, U.K., <http://www.vectorlabs.com>; catalog no. H1500) and coverslipped.

A panel of 16 primary antibodies that recognize the corresponding canine genes was used: rabbit anti-Msx2 (1:200) (CeMines, Golden, CO; catalog no. AB/HD19), rabbit anti-Sox10 (1:100) (CeMines; catalog no. AB/HMG4), mouse anti-Nes (1:200) (BD Biosciences, San Diego, CA, <http://www.bdbiosciences.com>; catalog no. 61158), goat anti-Myo10 (1:200) (Santa Cruz Biotechnology Inc., Santa Cruz, CA, <http://www.scbt.com>; catalog no. SC-23137), mouse anti-Ets1 (1:200) (Santa Cruz Biotechnology Inc.; catalog no. SC-56674), rabbit anti-Adam12 (1:200) (Santa Cruz Biotechnology Inc.; catalog no. SC-25579), goat anti-Crmp1 (1:200) (Santa Cruz Biotechnology Inc.; catalog no. SC-46872), goat anti-Cryab (1:200) (Santa Cruz Biotechnology Inc.; catalog no. SC-22391), goat anti-Ube4b/Ufd2 (1:200) (Santa Cruz Biotechnology Inc.; catalog no. sc 22391), goat anti-Thop1 (1:200) (Santa Cruz Biotechnology Inc.; catalog no. sc 30579), mouse anti-Oct4 (Santa Cruz Biotechnology Inc.; catalog no. sc 5279), rabbit anti-Sox2 (StemCell Technologies, Vancouver, BC, Canada, <http://www.stemcell.com>; catalog no. 1438), mouse anti-Klf4 (Abcam, Cambridge, U.K., <http://www.abcam.com>; catalog no. ab75486), mouse anti-c-Myc (Abcam; catalog no. ab32), mouse anti-Nanog (Abnova, Taipei, Taiwan, <http://www.abnova.com>; catalog no. H00079923-M02), and rabbit anti-Lin28 (Abcam; catalog no. ab 46020).

The following secondary antibodies were used: DyLight 594-conjugated goat anti-rabbit IgG (Jackson Laboratory, Newmarket, U.K., <http://www.jax.org>; catalog no. 111-515-144), DyLight 488-conjugated goat anti-rabbit IgG (Jackson; catalog no. 111-485-144), DyLight 594-conjugated goat anti-mouse IgG (Jackson; catalog no. 115-515-146), DyLight 488-conjugated goat anti-mouse IgG (Jackson; catalog no. 115-485-146), and DyLight 488-conjugated donkey anti-goat IgG (Jackson; catalog no. 105-485-147). These secondary antibodies are designed for multiple labeling and have been used successfully in the past [11].

Quantitative analysis was performed on five dogs. For each antibody on the panel, cells were scored in 10 random fields of vision. Strongly immunoreactive cells were expressed as percentage of total. Weakly immunopositive cells were excluded from analysis. AxioVision LE software (V4.8.2.0, 2010; Carl Zeiss Micro-Imaging GmbH, Jena, Germany, <http://www.zeiss.com>) was used, and statistical analysis was conducted using Microsoft Excel 2008 (version 12.1.3; Microsoft, Redmond, WA, <http://www.microsoft.com>). For each dog, a mean percentage of positive cells was calculated, averaging positive cells from the 10 random fields of vision. The final result was expressed as the mean of the individual mean percentages of positive cells of the five dogs plus or minus the SEM.

Clonal Cultures

After 5 days of ex vivo expansion, cells were detached with TrypLE and seeded at clonal density of 25 cells per plate onto CellStart-coated 35-mm plates. After 18 hours, individual cells were circled

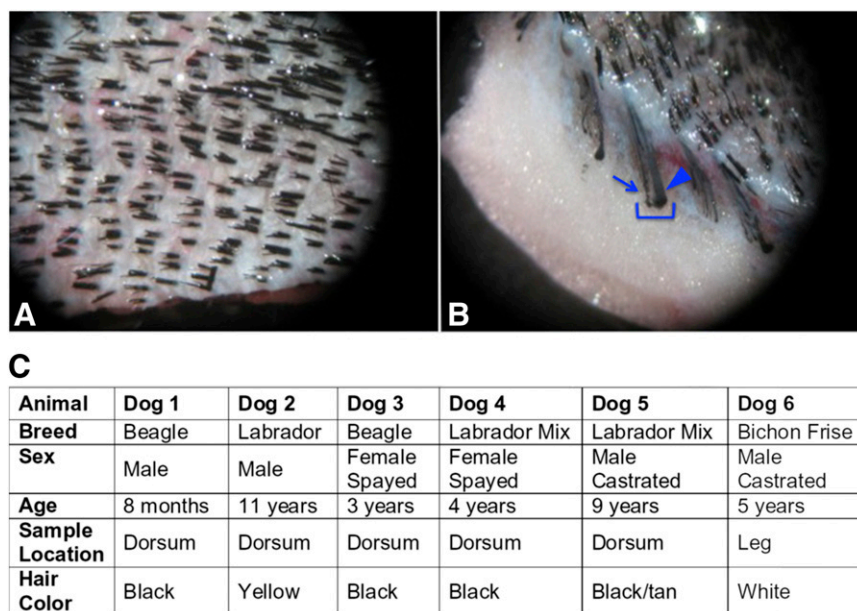


Figure 1. Anatomy of canine hair. **(A):** Dorsal view of canine haired skin. Skin is from an adult male castrated Dachshund. Representative image of canine haired skin. Note that each follicular unit has multiple hair shafts exiting through one follicular opening. **(B):** En face view of canine haired skin in **(A)** showing the anatomy of a compound hair (bracket). The primary hair (arrowhead) is prominent and surrounded by several smaller secondary hairs (e.g., arrow). **(C):** Dogs included in this study. Canine epidermal neural crest stem cells were isolated from all dogs.

with a diamond-tipped circle scribe of 4-mm diameter. Single cells in circles that overlapped with another circle and doublets were excluded from the analysis. The cell suspensions consisted of >90% single cells.

To drive differentiation into the cell types of interest, the culture medium was supplemented with pertinent growth factors. Differentiation into chondrocytes was promoted by supplementation with 10 ng/ml bone morphogenetic protein 2 (BMP2; R&D Systems; catalog no. 355-BEC/CF). For differentiation into neuronal cells, the culture medium consisted of NeuroCult NSA (StemCell Technologies; catalog no. 05750), Supplement B 27 (Invitrogen; #12587-10), 1% (vol/vol) FBS, 10 ng/ml rhEGF2 (R&D Systems; catalog no. 233FB/CF), 20 ng/ml rhEGF (R&D Systems; catalog no. 236EG/CF), 5 ng/ml canine SCF (Kingfisher Biotech, St. Paul, MN, <http://www.kingfisherbiotech.com>; catalog no. RPO154D-005), 10 ng/ml rhNT-3 (R&D Systems; catalog no. 267N3/CF), GlutaMAX (1:100), penicillin/streptomycin (1:100), and 2.5 μ g/ml amphotericin B (1:100), 20 ng/ml nerve growth factor (R&D Systems; catalog no. 356-GF/CF), 1 ng/ml transforming growth factor- β 2 (R&D Systems; catalog no. 302-B2/CF), and 100 μ M dibutyryl cAMP (Sigma-Aldrich; catalog no. D0260). For Schwann cell differentiation, the culture medium consisted of NeuroCult NSA (StemCell Technologies; catalog no. 05750), supplement B27 (Invitrogen; catalog no. 12587-10), 1% (vol/vol) FBS, 10 ng/ml rhEGF2 (R&D Systems; catalog no. 233FB/CF), 20 ng/ml rhEGF (R&D Systems; catalog no. 236EG/CF), 5 ng/ml canine SCF (Kingfisher Biotech; catalog no. RPO154D-005), 10 ng/ml rhNT-3 (R&D Systems; catalog no. 267N3/CF), GlutaMAX (1:100), penicillin/streptomycin (1:100), 2.5 μ g/ml amphotericin B (1:100), 10 nM neuregulin 1 (R&D Systems; catalog no. 377-HB/CF), and 10 ng/ml ciliary neurotrophic factor (R&D Systems; catalog no. 257-NT/CF).

After 8–15 days in differentiation medium, cultures were fixed with 4% paraformaldehyde for 30 minutes and processed for indirect immunocytochemistry as described previously. The

following cell type-specific primary antibodies were used: goat anti-collagen type II (1:200) (Abcam; catalog no. ab24128), mouse anti-smooth muscle actin (1:200) (Sigma-Aldrich; catalog no. A5228), mouse anti- β -III tubulin (1:200) (Millipore, Billerica, MA, <http://www.millipore.com>; catalog no. MAB1637), and rabbit glial fibrillary acidic protein (GFAP; 1:1,000) (Abcam; catalog no. ab7260).

To determine self-renewal capability of cEPI-NCSC, serial cloning was performed. Clones were subcloned using sterile cloning rings that were dipped into sterile vacuum grease to provide a seal and then placed on top of the clone. Subsequently, the clone was rinsed twice with 3 drops of calcium- and magnesium-free PBS each, and finally 3 drops of TrypLE were added. The cells were reseeded on 35-mm plates at clonal density (25 cells per 35-mm plate). Subclones were incubated for up to 3 weeks and subsequently analyzed by indirect immunocytochemistry, as detailed, for primary clones.

RESULTS

Bulge Explants, Isolation, and Expansion of cEPI-NCSC

In contrast to humans and rodents, dogs have compound hair follicles that contain one large primary hair and several smaller secondary hairs (Fig. 1A, 1B). We isolated and cultured explants from both hair types individually. cEPI-NCSC were isolated from several dog breeds, from both sexes, and from two different locations of the body, the dorsum and the leg. The ages of the dogs ranged from 8 months to 11 years. Hair color varied, including white, yellow, tan, brown, and black (Fig. 1C). Cells emigrated from hair follicular explants from both primary and secondary hairs within 6 days after explantation from all dog breeds tested (Fig. 2A). The cells had stellate morphology characteristic of neural crest cells (Fig. 2B). Explants from primary hair follicles resulted in

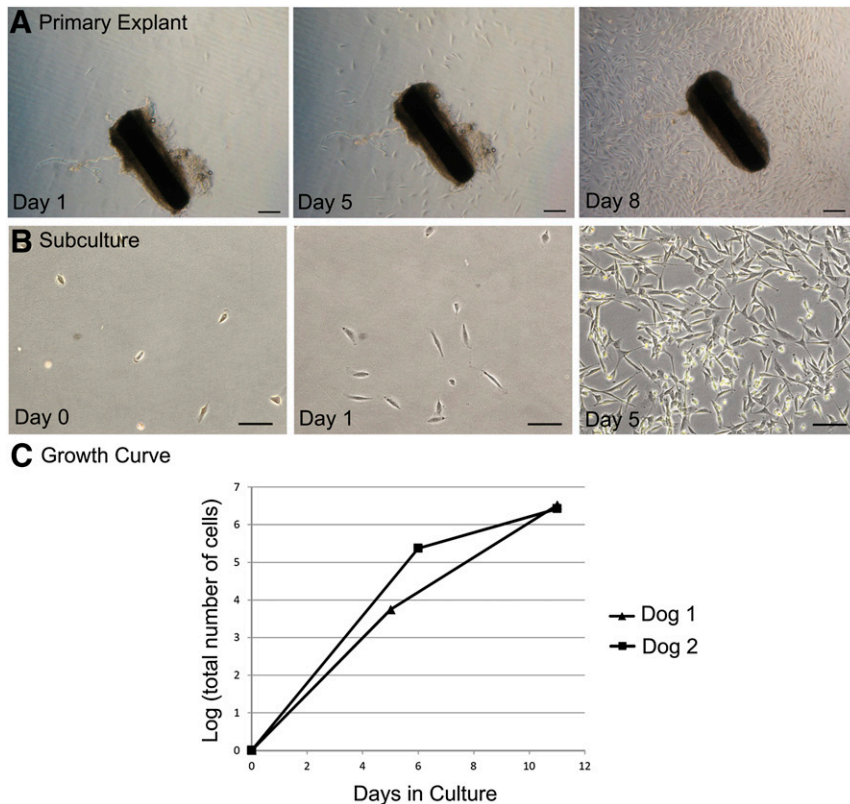


Figure 2. Bulge explant culture and ex vivo expansion. **(A):** Time course of ex vivo expansion of canine epidermal neural crest stem cells (cEPI-NCSC) from a primary hair follicle (dog 4: phase contrast optics). Scale bars = 400 μm . **(B):** cEPI-NCSC short-term ex vivo expansion, representative image. Cells start to divide less than 24 hours after plating. Millions of cells are obtained from one bulge explant by day 5 of ex vivo expansion (dog 3: phase contrast optics). Scale bars = 200 μm . **(C):** cEPI-NCSC growth curve during ex vivo expansion. On average, 3 million cells were obtained per hair follicle within 11 days after explantation.

cEPI-NCSC emigration from an average of $11.11 \pm 3.18\%$ of cultured explants, whereas explants from secondary hair follicles from the same dogs resulted in an average emigration of $16.66 \pm 3.33\%$. There was no significant difference between primary and secondary hair follicles in terms of the isolation efficiency of cEPI-NCSC ($n = 6$, $p = .133$). The low efficiency was likely related to the fact that shipped tissue was received several days after biopsies were taken.

To determine the feasibility of future cEPI-NCSC spinal grafts, we developed a protocol for ex vivo expansion of cEPI-NCSC (Fig. 2B). The main goal was to obtain high numbers of stem cells within a short period of time in culture in order to maintain genomic integrity. cEPI-NCSC grew exponentially (Fig. 2C). On average, 3 million cells were obtained per hair follicle within 11 days following explantation, the time point used for experimentation. After 11 days, the cells continued to grow logarithmically for a prolonged period of time (data not shown).

Design and Validation of Reagents for the Dog Species

Tools to detect markers specific for the dog are not yet widely available. Consequently, we developed and validated dog-specific primer sets to characterize the neural crest origin of cEPI-NCSC (supplemental online Table 1). cDNA from different canine tissues and from cEPI-NCSC was used to evaluate differences in expression between various tissues by RT-PCR (Fig. 3A). As expected cEPI-NCSC and whole embryo tissue expressed all molecular

signature genes and other neural crest markers, as well as *Nes*. In contrast, other tissues expressed subsets of these markers only. Similarly, primer sets to evaluate expression of pluripotency markers were developed. cDNA from whole embryo and from cEPI-NCSC was used to test the primer sets (Fig. 4A). The PCR product size and melting temperature were designed to be optimal for qPCR, with a PCR product size of 100–200 base pairs and a melting temperature of 60°C.

Neural Crest Origin

We used the above discussed primer pairs to verify, by qPCR, the gene expression profile in cEPI-NCSC. *Msx2*, *Thop1*, *Myo10*, *Ets1*, *Adam12*, *Crmp1*, *Ube4b*, and *Cryab* were detected by qPCR and were expressed at 71%–99% relative to the average of the three housekeeping genes. The neural crest origin was further demonstrated with the general neural crest markers *Sox10* (62%) and *Snai2* (84%). The progenitor cell marker *Nes* was also expressed (81%) (Fig. 3B).

Marker expression was then tested at the protein level by indirect immunocytochemistry. The great majority of cEPI-NCSC expressed NCSC signature markers as well as *Sox10* and *Nes* at the protein level (Fig. 5). The transcription factor *Ets1* was expressed in $94.4 \pm 0.6\%$ cells with nuclear to perinuclear location. The metalloproteinase *Thop1* was expressed in the cytoplasm of $99.8 \pm 0.1\%$ cells. The transcriptional repressor protein *Msx2* was expressed in the cytoplasm of $97.1 \pm 0.7\%$ cells. *Crmp1*, a cytosolic phosphoprotein

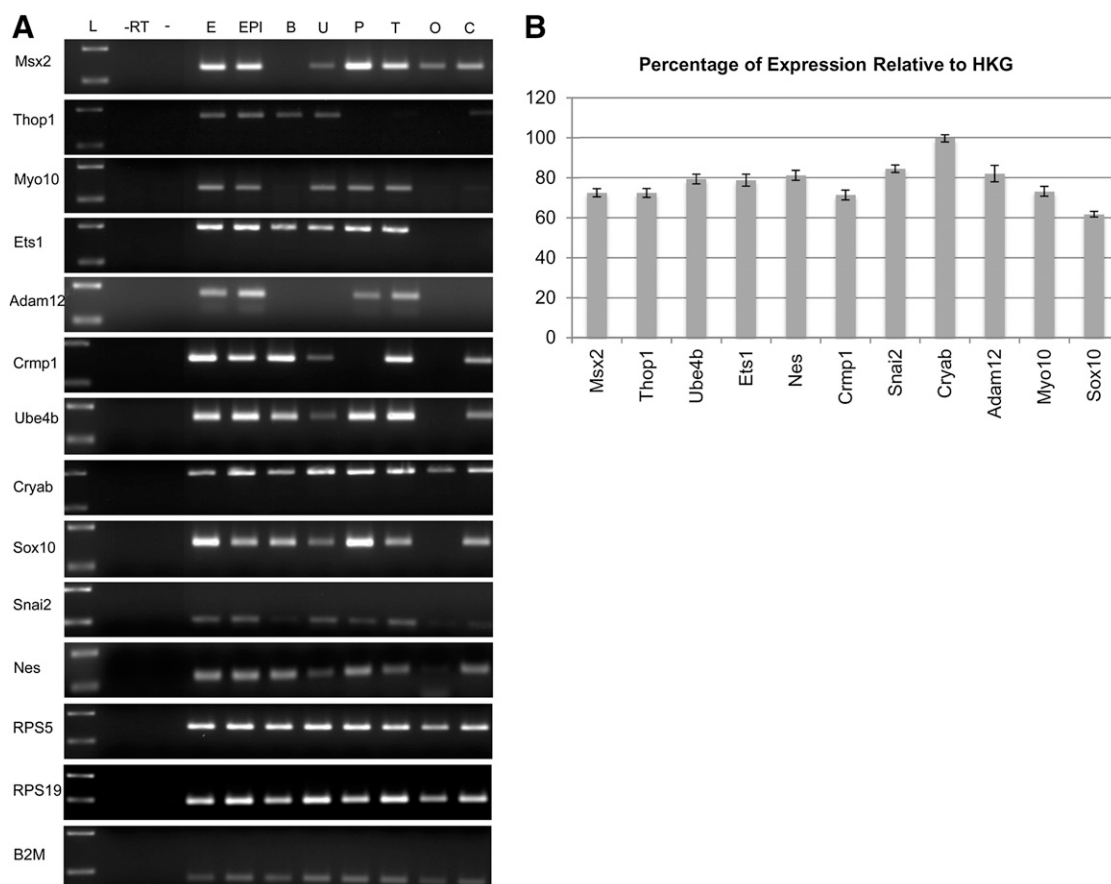


Figure 3. Comparative analysis of neural crest stem cell markers. **(A):** Neural crest marker gel electrophoresis of reverse transcriptase polymerase chain reaction results. Test of canine epidermal neural crest stem cell (cEPI-NCSC) molecular characterization and housekeeping primer sets in different dog tissues. **(B):** cEPI-NCSC gene expression levels relative to HKGs after ex vivo expansion. Percentage of relative expression by quantitative reverse transcriptase polymerase chain reaction of selected molecular signature genes (Msx2, Thop1, Ube4b, Ets1, Crmp1, Cryab, Adam12, Myo10), general neural crest stem cell genes (Snai2, Sox10), and a general stem cell gene (Nes). Data are from five donors with exception of Sox10 ($n = 4$). Abbreviations: -, water; -RT, minus reverse transcriptase control; B, brain; C, colon; E, embryo; EPI, canine epidermal neural crest stem cells; HKG, housekeeping gene; L, standard, 100–200 base pairs; O, ovary; P, placenta; T, testicle; U, uterus.

expressed exclusively in the nervous system, was expressed in the cytoplasm of $98.4 \pm 0.8\%$ cells. The ubiquitination protein Ube4b was expressed in the cytoplasm of $95.4 \pm 0.6\%$ of the cells. Myo10 expression was cytoplasmic and observed in $96.8 \pm 0.3\%$ of the cells. The disintegrin and metalloprotease protein Adam12 had cytoplasmic expression in $89.2 \pm 0.9\%$ of the cells. The expression of the crystallin Cryab was cytoplasmic in $98.9 \pm 0.3\%$ of the cells. The neural crest marker Sox10 had cytoplasmic expression in $98.3 \pm 0.4\%$ of the cells. The general stem cell marker Nes, an intermediate filament, was observed in the cytoplasm of $94.9 \pm 2.0\%$ of the cells. Together, the data indicate that cEPI-NCSC are of neural crest origin.

Interestingly, like hEPI-NCSC, cEPI-NCSC expressed the essential pluripotency genes (Fig. 4). At the RNA level, expression of Oct4, Sox2, Klf4, c-Myc, and Lin28 varied between 59% and 89% relative to the average of the three housekeeping genes (Fig. 4B). Pluripotency marker expression was additionally tested at the protein level by indirect immunofluorescence. The transcription factor Oct4 was expressed in $89.7 \pm 1.4\%$ cells with cytoplasmic and nuclear location. The transcription factor Sox2 was expressed in $91.0 \pm 2.1\%$ cells with cytoplasmic and nuclear location. The transcription factor Klf4 was expressed in $93.6 \pm 2.2\%$ cells with cytoplasmic and nuclear location. The proto-oncogene

c-Myc was expressed in the cytoplasm of $96.6 \pm 0.5\%$ cells. Notably, as in hEPI-NCSC (unpublished data), c-Myc immunoreactivity was never observed in the nucleus, suggesting that cEPI-NCSC are not tumorigenic. Lin28 was strongly expressed in the cytoplasm of $96.6 \pm 0.7\%$ cells. The transcription factor Nanog had cytoplasmic to perinuclear location in $92.5 \pm 0.4\%$ of cells.

Together, these data characterize, at the RNA and protein levels, cEPI-NCSC as cells from neural crest origin that reside in the middle area of canine primary and secondary hair follicles. Moreover, similar to hEPI-NCSC, cEPI-NCSC express pluripotency genes.

Multipotency and Self-Renewal

Multipotency and self-renewal ability were determined in vitro by clonal analysis and serial cloning, respectively. cEPI-NCSC were seeded at clonal density (25 cells per 35-mm plate). In clonal culture, a total of 40 single cells were marked 18 hours after cloning and then cultured for 18 days. The majority of clone-forming cells, $72.5 \pm 7.06\%$, generated colonies composed of highly proliferative cells (Fig. 6). A clone-forming cell is marked at 18 hours after seeding (Fig. 6A). By days 2 and 3, the same clone consisted of four and six daughter cells, respectively. Cells continued to proliferate logarithmically, and by day 9, clones consisted of thousands of

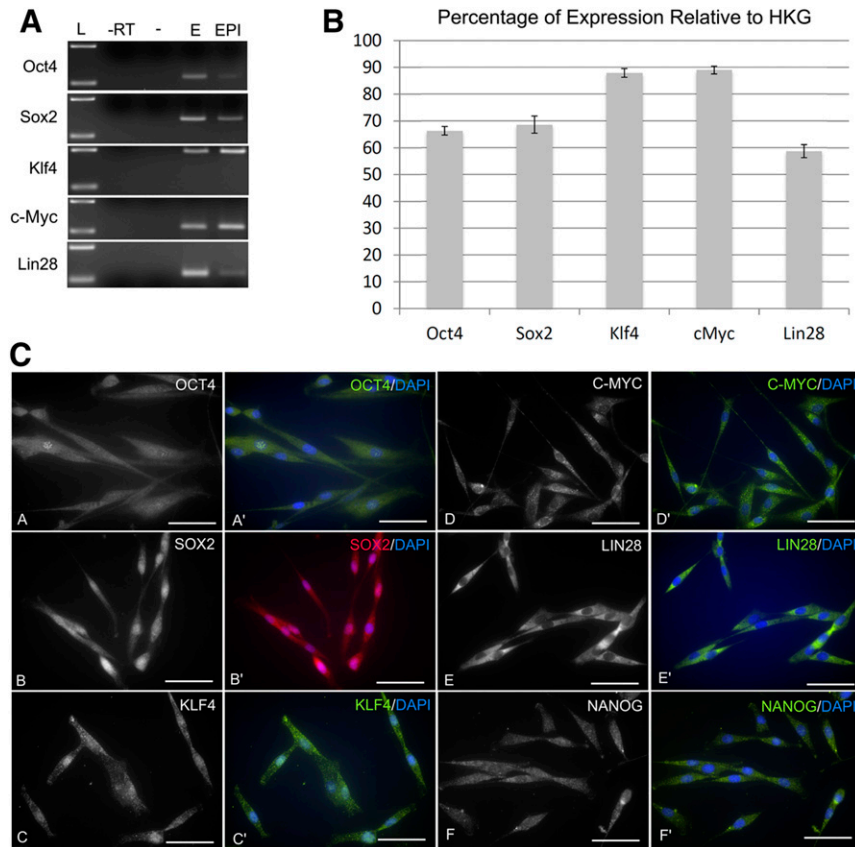


Figure 4. Pluripotency marker expression. **(A):** Test of canine epidermal neural crest stem cell (cEPI-NCSC) molecular characterization primer sets. **(B):** cEPI-NCSC gene expression after ex vivo expansion. Percentage of relative expression by quantitative reverse transcriptase polymerase chain reaction of pluripotency genes; data from four donors. **(C):** Characterization at the protein level by immunocytochemistry. cEPI-NCSC show immunofluorescence for the pluripotency markers Oct4 (images A, A'), Sox2 (images B, B'), Klf4 (images C, C'), c-Myc (images D, D'), Lin28 (images E, E'), and Nanog (images F, F'). Blue, DAPI nuclear stain. Data are from five donors. Scale bars = 50 μ m. Abbreviations: -, water; -RT, minus reverse transcriptase; DAPI, 4',6-diamidino-2-phenylindole; E, embryo; EPI, canine epidermal neural crest stem cells; HKG, housekeeping gene; L, standard, 100–200 base pairs.

cells (Fig. 6E, 6F). The remaining single cells did not divide ($5 \pm 3.44\%$), died ($7.5 \pm 4.16\%$), or formed clones composed of only two to four cells ($7.5 \pm 4.16\%$).

Double staining with cell type-specific antibodies, performed after differentiation, showed that clones contained multiple cell types. Clones that contained smooth muscle actin immunoreactive myofibroblasts also contained collagen type II chondrocytes (Fig. 7A, images A–A'), β -III tubulin immunoreactive neuroblasts (Fig. 7A, images B–B'), or GFAP-positive putative Schwann cells (Fig. 7A, images C–C'). Clones that contained GFAP-positive cells also contained β -III tubulin-immunoreactive cells (Fig. 7A, images D–D'). The observation of multiple cell types in clones shows that the majority of cells emigrating from hair follicle explants are multipotent. Furthermore, the data demonstrate that cEPI-NCSC can give rise to all major neural crest derivatives, including chondrocytes, neuronal cells, smooth muscle cells and myofibroblasts, and Schwann cells.

Self-renewal was determined by serial cloning. To this end, primary clones were resuspended 6 days after cloning. After plating, a total of 29 individual cells in clonal subculture were marked. Clone-forming ability was maintained, where $41.3 \pm 0.09\%$ of secondary clones consisted of highly proliferative cells. The remaining single cells did not divide ($6.8 \pm 0.04\%$), died ($13.79 \pm 0.06\%$), or formed clones composed of only two to four cells ($37.9 \pm 0.09\%$).

Double stains with cell-type-specific antibodies showed that secondary clones also contained multiple cell types. Subclones containing myofibroblasts also contained chondrocytes (Fig. 7B, images A–A'), Schwann cells (Fig. 7B, images B–B'), and neuroblasts (Fig. 7B, image C). The fact that secondary clones contained multiple distinct, differentiated cell types showed that the secondary clone-forming cells were multipotent cells. From this it follows that the original clone-forming cell was able to give rise to new multipotent cells, that is, to self-renew. Together, the clonal analyses showed that cEPI-NCSC fulfill the criteria for the definition of multipotent stem cells.

DISCUSSION

We showed that canine hair follicles contain multipotent neural crest-derived stem cells with features comparable to those in mice and humans [1, 2, 9, 11]. cEPI-NCSC can be expanded ex vivo into large numbers of stem cells within a short period of time. cEPI-NCSC can be obtained with equal efficiency from primary and secondary hair follicles. By taking advantage of the migratory ability of neural crest cells, cEPI-NCSC can be obtained as a highly pure population of multipotent stem cells without the need for purification. cEPI-NCSC are present in hair follicles from diverse locations of the body, in dogs of various breeds, and within a wide

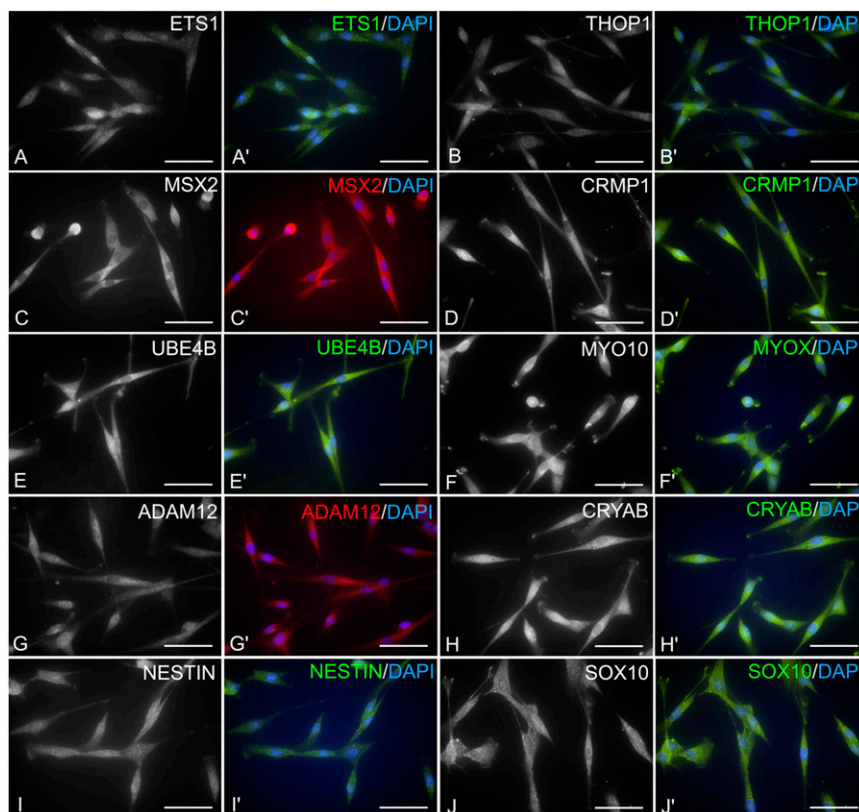


Figure 5. Characterization of canine epidermal neural crest stem cells (NCSC) by immunocytochemistry. Representative images. Canine epidermal NCSC express at the protein level NCSC signature genes, general neural crest markers, and a general stem cell marker. Images shown are the antibody-specific (black and white) and merged images (color) using DyLight 488- or DyLight 594-conjugated secondary antibodies. Blue, DAPI nuclear stain. **(A, A')**: Transcription factor Ets1 shows mainly nuclear immunoreactivity. **(B, B')**: Thop1 shows variable cytoplasmic immunoreactivity. **(C, C')**: Transcription factor Msx2 with mostly cytoplasmic immunoreactivity. **(D, D')**: Cytosolic protein Crmp1 has variable cytoplasmic expression. **(E, E')**: Ube4b shows strong cytoplasmic expression. **(F, F')**: Myo10 shows strong cytoplasmic immunoreactivity. **(G, G')**: Adam12, a membrane-anchored protein, shows variable cytoplasmic expression. **(H, H')**: Cryab has diffuse cytoplasmic immunoreactivity. **(I, I')**: The intermediate filament Nes shows cytoplasmic immunoreactivity. **(J, J')**: Sox10, a nucleo-cytoplasmic shuttle protein, shows mainly cytoplasmic immunoreactivity. Scale bars = 50 μ m. Abbreviation: DAPI, 4',6-diamidino-2-phenylindole.

age range. Finally, we provide novel tools for research into canine stem cells.

In contrast to humans and mice, dogs have compound hair follicles, in which multiple hair shafts, arising from primary and associated secondary follicles, exit through a common follicular ostium. Gurlt first described this compound nature of canine hair follicles in 1835 [29]. Hair follicles are unique biological structures in the sense that they undergo lifelong cycles of destruction and regeneration. This prompted researchers to suggest that hair follicles may be a fertile source of primitive cell populations that could be used in regenerative medicine [27, 30]. Through label retention studies, Cotsarelis et al. [31] described epidermal stem cells in the bulge of hair follicles, which generate new skin, hair, and sebaceous glands. The follicular bulge consists of a subpopulation of the outer root sheath and a stem cell niche that is located in the midportion of the follicle at the arrector pili muscle attachment site [32, 33]. There are few studies on the stem cell biology of canine hair follicles [27, 34, 35]. Comparable to hair in humans and mice, canine epidermal stem cell candidates also reside in the bulge region [34, 36, 37]. Considering this background knowledge, we targeted our dissections to the midfollicular area, the putative bulge equivalent, of primary and secondary hairs. Similar yields of cEPI-NCSC between primary and secondary hair follicles

indicate that both primary and secondary hair follicles possess a stem cell niche. Others have reported canine skin-derived neuroprogenitor cells, but the origin of these cells is unknown [38].

In order to characterize the cEPI-NCSC, we developed and validated novel dog-specific primer pairs for qPCR. Canine gene expression profiles across eight different canine tissues (Fig. 3A) were similar to published studies in human and mouse (European Molecular Biology Laboratory, European Bioinformatics Institute, <http://www.ebi.ac.uk>). Sox10 was detected in nearly all tissues tested. This is likely because of the presence of neural crest-derived Schwann cells in innervating nerves, as Schwann cells continue to express Sox10. Likewise, the detection of Snai2 in uterus, placenta, testicle, and colon may result from the persistence of pigment cell precursors or other neural crest-derived precursors in these organs. In particular, the enteric nervous system in the colon is highly likely to harbor neural crest-derived progenitor cells.

Using an approach analogous to establishing the existence of EPI-NCSC in humans, we have determined that the follicles of various breeds of dog, of different colors, and from different locations in the body contain multipotent stem cells of neural crest origin. Notably, we obtained cEPI-NCSC from a white dog as well. This was not necessarily expected because neural crest-derived pigment cells give hair its color; however, white-haired dogs are

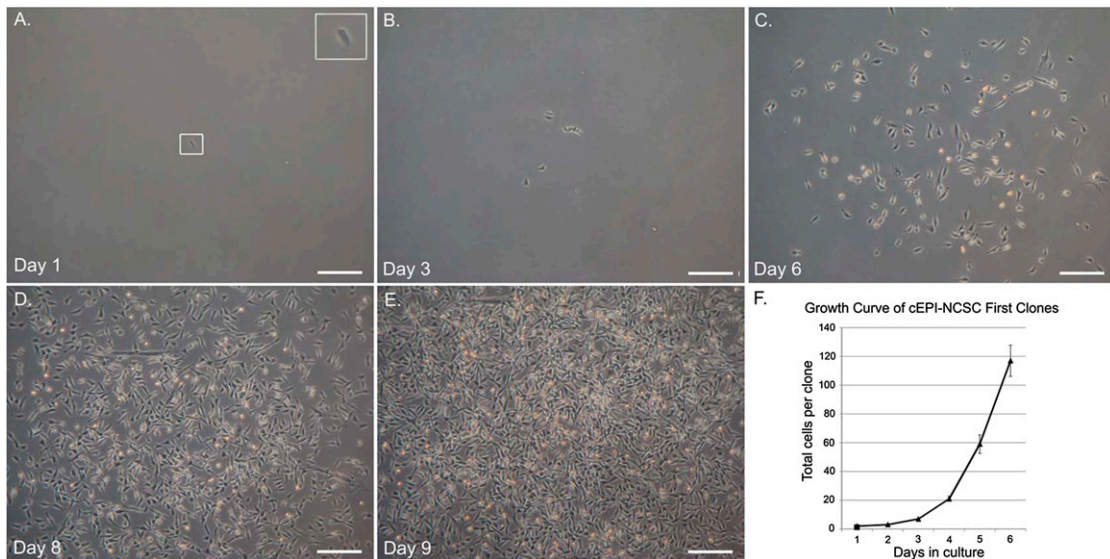


Figure 6. Clonal culture. Primary clone from haired skin of dog 1. **(A):** Clone-forming cell. Inset, clone-forming cell at higher magnification. **(B):** Six daughter cells of the same clone-forming cells at day 3. **(C–E):** Cells continued to proliferate, forming a clone consisting of thousands of cells by clonal culture day 9. **(F):** Growth curve of cells in clones showing exponential growth ($n = 29$). Abbreviation: cEPI-NCSC, canine epidermal neural crest stem cell.

not necessarily albino because, depending on the type of mutation, they can have pigmented skin. Moreover, white-haired dogs can develop melanomas [39]. cEPI-NCSC can be expanded *ex vivo* with a culture medium very similar to the medium used for hEPI-NCSC. Taken together, cEPI-NCSC have very similar characteristics to human and mouse EPI-NCSC. Consequently, we have laid the groundwork for the use of cEPI-NCSC in large animals. In addition to their potential for becoming a therapeutic tool for canine patients, cEPI-NCSC also offer the key advantage of being an important translational model for spontaneously occurring human SCI [24–26, 40–42].

Although originally *c-Myc*, *Oct4*, *Sox2*, *Klf4*, *Nanog*, and *Lin28* were thought to be transcription factors that are located in the nucleus only and limited to pluripotent cells, more recent research indicates a wider expression pattern. The spatiotemporal dynamic behavior of *Oct4* remains largely unknown, but a recent report showed that *Oct4* is a nucleocytoplasmic shuttling protein and thus can be present in the nucleus as well as in the cytoplasm [43]. *Sox2* expression is crucial for early development and maintenance of embryonic stem cells [44, 45]. *Sox2* protein expression has been localized to the nucleus and the cytoplasm [46]. In addition to being one of the key transcription factors used to reprogram cells into induced pluripotent stem cells [47], *Sox2* overexpression or gene amplification has also been associated with cancer development in several tissues such as lung, esophagus, and breast [44]. Previous studies about *Klf4* functions focused mainly on its role as a transcription factor; however, recent reports have studied the functions of *Klf4* in the cytoplasm and its role in regulating cytoskeletal organization [48, 49]. Originally it was believed that *Nanog* was expressed only in pluripotent cells. Recently, *Nanog* protein and its pseudogene forms have also been shown to play roles in a variety of cancer cell lines and tumors, including pancreatic carcinoma, breast cancer, ovarian cancer, and endometrial carcinoma [50–52]. A study of cervical cancer describes that *Nanog* is frequently expressed in the cytoplasm, instead of the nucleus, and its stromal distribution is related to

cancer progression [53]. *Lin28A* targets mRNAs destined for the endoplasmic reticulum and thus is located in the cytoplasm [54–56]. Altered cytoplasmic/nuclear distribution of the *c-Myc* protein has been previously described [57–60].

Intervertebral disk disease is one of the most common causes of SCI in dogs. Disk ruptures are observed in small, medium, and large-breed dogs but are most commonly observed in breeds predisposed to chondrodystrophy, such as the Dachshund, Pekinese, and Shih Tzu. Understanding the pathogenesis of the lesion is paramount to the development of effective therapeutic approaches. Recently, there has been an increasing number of studies focusing on the molecular basis of canine central nervous system disease [42]. In traumatic SCI caused by acute intervertebral disk extrusion, the primary injury is a mechanical trauma composed of concussive and contusive forces as well as compression of neural tissues. This is followed by a secondary cascade of destructive events. Primary and secondary events lead to tissue ischemia, necrosis, hemorrhage, excitotoxicity, apoptosis, and inflammation [61]. Similar to humans and in contrast to rodents, the second phase of canine SCI is characterized by robust reaction of microglia and macrophages with upregulation of major histocompatibility complex class II molecule expression and myelinophagia [41, 62, 63]. Consequently, canine SCI is a good model for human SCI.

Despite the large number of therapeutic alternatives for SCI, current canine clinical trials have not yet led to a major breakthrough [17]. Cell-based therapies are currently the focus in several canine experimental and clinical trials [64–74]. The different types of stem cells used in canine SCI include canine umbilical cord-derived mesenchymal stem cells (MSCs), canine Wharton's jelly-derived MSCs, canine adipose-derived MSCs, canine bone marrow-derived MSCs, human umbilical cord blood-derived MSCs, human neural stem cells, and canine olfactory ensheathing cells (OECs). The strength of EPI-NCSC resides in their close relationship to spinal cord progenitor cells [12]; the fact that they can give rise to spinal cord-specific cell types [13]; and the expectation that, unlike other types of stem cells, their epigenetic memory

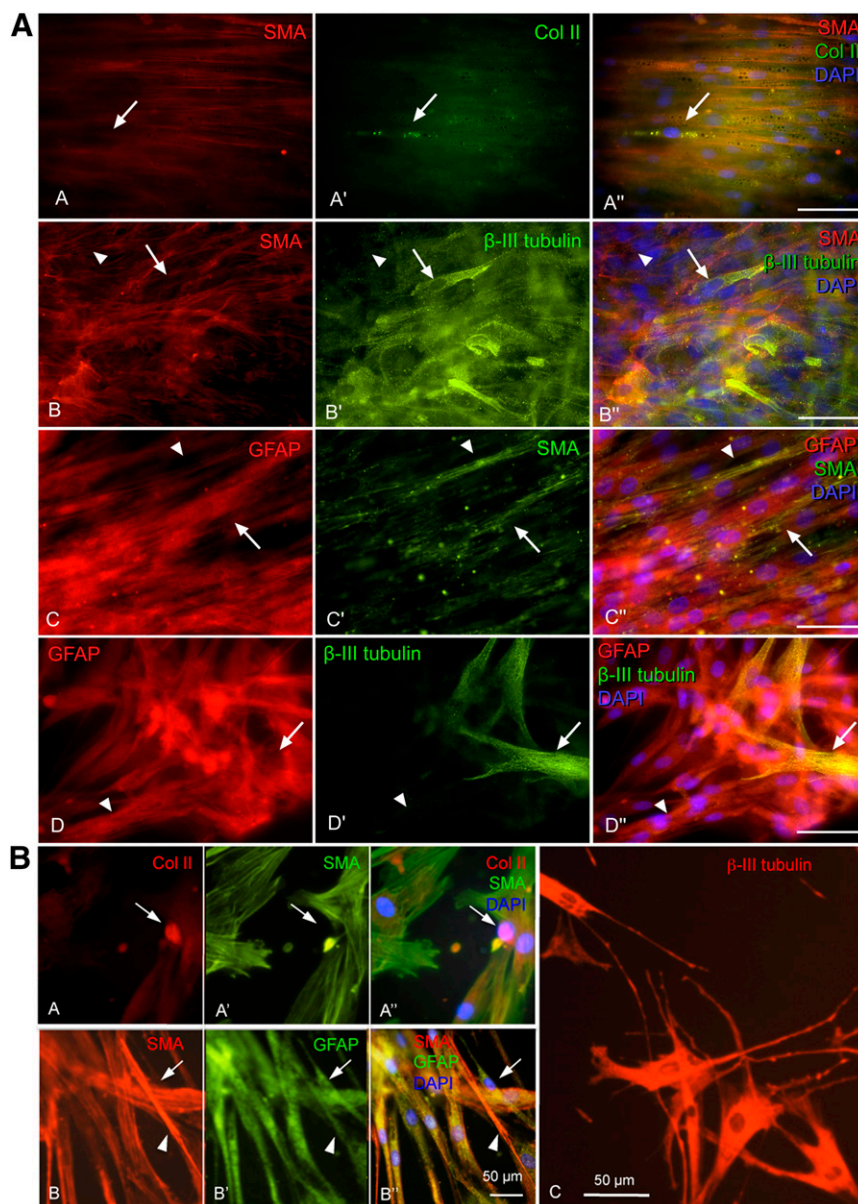


Figure 7. Indirect immunofluorescence of primary and secondary clones. Representative images. The clones were probed with cell-type-specific antibodies to determine whether primary and secondary clones contain more than one cell type. Triple stains combining two cell-type-specific antibodies (isolated red or green images) and merged image using DyLight 488- and DyLight 594-conjugated secondary antibodies and DAPI nuclear stain (blue). **(A):** Primary clones. Two cell types were observed within the clonal cultures. Immunoreactive COLII cell (image A', arrow) that is not reactive for SMA (image A). Immunoreactive SMA cell (image B, arrowhead) that is not reactive for β -III tubulin (image B'). Immunoreactive β -III-tubulin cell (arrow) that is mostly not reactive for SMA (image B). Immunoreactive GFAP cell (image C, arrow) that is not reactive for SMA (image C'). Immunoreactive SMA cell (image C', arrowhead) that is not reactive for GFAP (image C). GFAP-immunoreactive cell (image D, arrowhead) that is β -III tubulin immunonegative (image D'). Immunoreactive β -III tubulin (image D', arrow) cell that is not reactive for GFAP (image D). The data show that canine epidermal neural crest stem cells are multipotent. Scale bars = 50 μ m. **(B):** Secondary clones. Representative images. Immunocytochemistry combining two cell-type-specific antibodies using DyLight 488-conjugated (green fluorescence) and DyLight 594-conjugated (red fluorescence) secondary antibodies and DAPI nuclear stain (blue). Two cell types were observed within the secondary clonal cones. Immunoreactive COLII cell (image A, arrow) that is not reactive for SMA (image A', arrow). Immunoreactive SMA cell (image B, arrowhead) that is not reactive for GFAP (image B', arrowhead). Immunoreactive GFAP cell (image B', arrow) that is not reactive for SMA (image B, arrow). Immunoreactive β -III tubulin cells (image C). These results show that canine epidermal neural crest stem cells can undergo self-renewal. Scale bars = 50 μ m. Abbreviations: Col II, collagen type II; DAPI, 4',6-diamidino-2-phenylindole; GFAP, glial fibrillary acidic protein; SMA, smooth muscle actin.

is closely related to that of spinal cord cells. In contrast to other cells, EPI-NCSC can be isolated as a virtually pure population of stem cells without the need for purification. In contrast, MSCs are a relatively heterogeneous population of cells that exhibit differences in molecular phenotype and differentiation potential,

depending on their source of origin [75]. OECs isolated from the canine olfactory bulb were shown to promote axon regeneration and remyelination in a rodent model and may have a promising effect in canine spontaneous SCI [40, 74]. Although autologous therapy with OECs is possible, their harvesting from

the olfactory bulb is rather invasive, whereas cEPI-NCSC can be obtained with a simple skin punch biopsy. Overall, cEPI-NCSC have various desirable characteristics that make them attractive candidates for cell-based therapies.

CONCLUSION

This study sets the stage for future studies in dogs. We have identified and characterized canine EPI-NCSC, and we have provided protocols for their isolation and ex vivo expansion. We characterized the cEPI-NCSC and verified their neural crest origin. cEPI-NCSC can generate all major neural crest derivatives. In vitro clonal analyses demonstrated multipotency and self-renewal capability of cEPI-NCSC. Together, these results fulfill the criteria of a multipotent stem cell. Furthermore, we provide novel primer sequences suitable for qPCR with dog tissue. Finally, we have reviewed the literature on stem cell therapy for canine SCI and discussed the major advantages of cEPI-NCSC relative to other types of stem cells already in use. Thus, we provided the groundwork for the development of a novel therapy for a condition with extremely poor prognosis and no available effective treatment.

ACKNOWLEDGMENTS

This project was supported by Medical Research Council Grant 22358, U.K. (M.S.-B.); the Center for Equine Health, UC-Davis (B.G.); a gift from Dick and Carolyn Randall (J.A.N., D.L.B., B.G.);

and Fundacao para a Ciencia e a Tecnologia, Ministerio da Educao e Ciencia, Portugal, under the Individual Doctoral Grant SFRH/ BD/ 64871/2009 (B.G.). We thank the owners of the dogs for donating skin samples, the members of the Nolta Laboratory for their excellent technical support, and Alla Narytnyk in the Sieber-Blum laboratory for her help.

AUTHOR CONTRIBUTIONS

B.G.: conception and design, financial support, collection and assembly of data, data analysis and interpretation, manuscript writing; J.S.A.: conception and design, data analysis and interpretation; G.M.: administrative support, collection and assembly of data; D.L.B.: conception and design, provision of study material and patients, financial support, data analysis and interpretation, final approval of manuscript; B.K.S.: conception and design, provision of study material and patients, collection and assembly of data, data analysis and interpretation, final approval of manuscript; J.A.N.: conception and design, financial support, data analysis and interpretation, final approval of manuscript; M.S.-B.: conception and design, financial support, data analysis and interpretation, manuscript writing, final approval of manuscript.

DISCLOSURE OF POTENTIAL CONFLICTS OF INTEREST

The authors indicate no potential conflicts of interest.

REFERENCES

- 1 Sieber-Blum M, Grim M. The adult hair follicle: Cradle for pluripotent neural crest stem cells. *Birth Defects Res C Embryo Today* 2004; 72:162–172.
- 2 Sieber-Blum M, Grim M, Hu YF et al. Pluripotent neural crest stem cells in the adult hair follicle. *Dev Dyn* 2004;231:258–269.
- 3 Hall BK, Gillis JA. Incremental evolution of the neural crest, neural crest cells and neural crest-derived skeletal tissues. *J Anat* 2013;222:19–31.
- 4 Dupin E, Sommer L. Neural crest progenitors and stem cells: From early development to adulthood. *Dev Biol* 2012;366:83–95.
- 5 Le Douarin N, Kalcheim C. *The Neural Crest (Developmental and Cellular Biology Series)*. 2nd ed. Cambridge, U.K.: Cambridge University Press, 1999.
- 6 Hall BK. *The Neural Crest and Neural Crest Cells in Vertebrate Development and Evolution*. 2nd ed. New York, NY: Springer, 2010.
- 7 Dupin E, Coelho-Aguiar JM. Isolation and differentiation properties of neural crest stem cells. *Cytometry A* 2013;83:38–47.
- 8 Richardson MK, Sieber-Blum M. Pluripotent neural crest cells in the developing skin of the quail embryo. *Dev Biol* 1993;157:348–358.
- 9 Hu YF, Zhang ZJ, Sieber-Blum M. An epidermal neural crest stem cell (EPI-NCSC) molecular signature. *STEM CELLS* 2006;24:2692–2702.
- 10 Rendl M, Lewis L, Fuchs E. Molecular dissection of mesenchymal-epithelial interactions in the hair follicle. *PLoS Biol* 2005;3:e331.
- 11 Clewes O, Narytnyk A, Gillinder KR et al. Human epidermal neural crest stem cells (hEPI-NCSC)—characterization and directed differentiation into osteocytes and melanocytes. *Stem Cell Rev* 2011;7:799–814.
- 12 Mujtaba T, Mayer-Proschel M, Rao MS. A common neural progenitor for the CNS and PNS. *Dev Biol* 1998;200:1–15.
- 13 Sieber-Blum M, Schnell L, Grim M et al. Characterization of epidermal neural crest stem cell (EPI-NCSC) grafts in the lesioned spinal cord. *Mol Cell Neurosci* 2006;32:67–81.
- 14 Hu YF, Gourab K, Wells C et al. Epidermal neural crest stem cell (EPI-NCSC)—mediated recovery of sensory function in a mouse model of spinal cord injury. *Stem Cell Rev* 2010;6:186–198.
- 15 Sieber-Blum M. Epidermal neural crest stem cells and their use in mouse models of spinal cord injury. *Brain Res Bull* 2010;83:189–193.
- 16 Gensel JC, Donnelly DJ, Popovich PG. Spinal cord injury therapies in humans: An overview of current clinical trials and their potential effects on intrinsic CNS macrophages. *Expert Opin Ther Targets* 2011;15:505–518.
- 17 Olby N. The pathogenesis and treatment of acute spinal cord injuries in dogs. *Vet Clin North Am Small Anim Pract* 2010;40:791–807.
- 18 Rossignol S, Frigon A. Recovery of locomotion after spinal cord injury: Some facts and mechanisms. *Annu Rev Neurosci* 2011;34:413–440.
- 19 Kwon BK, Sekhon LH, Fehlings MG. Emerging repair, regeneration, and translational research advances for spinal cord injury. *Spine (Phila Pa 1976)* 2010;35(suppl):S263–S270.
- 20 Tohda C, Kuboyama T. Current and future therapeutic strategies for functional repair of spinal cord injury. *Pharmacol Ther* 2011;132:57–71.
- 21 Donnelly EM, Lamanna J, Boulis NM. Stem cell therapy for the spinal cord. *Stem Cell Res Ther* 2012;3:24.
- 22 Bock P, Spitzbarth I, Haist V et al. Spatiotemporal development of axonopathy in canine intervertebral disc disease as a translational large animal model for nonexperimental spinal cord injury. *Brain Pathol* 2013;23:82–99.
- 23 Jeffery ND, Hamilton L, Granger N. Designing clinical trials in canine spinal cord injury as a model to translate successful laboratory interventions into clinical practice. *Vet Rec* 2011;168:102–107.
- 24 Jeffery ND, Smith PM, Lakatos A et al. Clinical canine spinal cord injury provides an opportunity to examine the issues in translating laboratory techniques into practical therapy. *Spinal Cord* 2006;44:584–593.
- 25 Smith PM, Jeffery ND. Histological and ultrastructural analysis of white matter damage after naturally-occurring spinal cord injury. *Brain Pathol* 2006;16:99–109.
- 26 Levine JM, Levine GJ, Porter BF et al. Naturally occurring disk herniation in dogs: An opportunity for pre-clinical spinal cord injury research. *J Neurotrauma* 2011;28:675–688.
- 27 Mecklenburg L, Linek M, Tobin DJ. *Hair Loss Disorders in Domestic Animals*. Hoboken, NJ: Wiley-Blackwell, 2009.
- 28 Brinkhof B, Spee B, Rothuizen J et al. Development and evaluation of canine reference genes for accurate quantification of gene expression. *Anal Biochem* 2006;356:36–43.
- 29 Gurll EF. *Vergleichende Untersuchungen über die Haut des Menschen und der Haus-Säugethiere, besonders in Beziehung auf die Absonderungsorgane des Haut-talgdes und des Schweisses*. Berlin, Germany: Arch F. Anat. Physiol u. Weissensch. Med, 1835:399–418.
- 30 Fuchs E. Beauty is skin deep: The fascinating biology of the epidermis and its appendages. *Harvey Lect* 1998-1999;94:47–77.
- 31 Cotsarelis G, Sun TT, Lavker RM. Label-retaining cells reside in the bulge area of pilosebaceous unit: Implications for follicular stem

cells, hair cycle, and skin carcinogenesis. *Cell* 1990;61:1329–1337.

32 Madsen A. Studies on the “bulge” (Wulst) in superficial basal cell epitheliomas. *Arch Dermatol* 1964;89:698–708.

33 Leshin B, White WL. Folliculocentric basaloid proliferation. The bulge (der Wulst) revisited. *Arch Dermatol* 1990;126:900–906.

34 Kobayashi T, Iwasaki T, Amagai M et al. Canine follicle stem cell candidates reside in the bulge and share characteristic features with human bulge cells. *J Invest Dermatol* 2010;130:1988–1995.

35 Ohyama M, Kobayashi T. Isolation and characterization of stem cell-enriched human and canine hair follicle keratinocytes. *Methods Mol Biol* 2012;879:389–401.

36 Kobayashi T, Shimizu A, Nishifuji K et al. Canine hair-follicle keratinocytes enriched with bulge cells have the highly proliferative characteristic of stem cells. *Vet Dermatol* 2009;20:338–346.

37 Sieber-Blum M, Hu Y. Epidermal neural crest stem cells (EPI-NCSC) and pluripotency. *Stem Cell Rev* 2008;4:256–260.

38 Valenzuela MJ, Dean SK, Sachdev P et al. Neural precursors from canine skin: A new direction for testing autologous cell replacement in the brain. *Stem Cells Dev* 2008;17:1087–1094.

39 Alhaidari Z, Olivry T, Ortonne JP. Melanocytogenesis and melagenesis: Genetic regulation and comparative clinical diseases. *Vet Dermatol* 1999;10:3–16.

40 Smith PM, Lakatos A, Barnett SC et al. Cryopreserved cells isolated from the adult canine olfactory bulb are capable of extensive remyelination following transplantation into the adult rat CNS. *Exp Neurol* 2002;176:402–406.

41 Boekhoff TM, Ensinger EM, Carlson R et al. Microglial contribution to secondary injury evaluated in a large animal model of human spinal cord trauma. *J Neurotrauma* 2012;29:1000–1011.

42 Bock P, Spitzbarth I, Haist V et al. Spatiotemporal development of axonopathy in canine intervertebral disc disease as a translational large animal model for nonexperimental spinal cord injury. *Brain Pathol* 2013;23:82–99.

43 Oka M, Moriyama T, Asally M et al. Differential role for transcription factor Oct4 nucleocytoplasmic dynamics in somatic cell reprogramming and self-renewal of embryonic stem cells. *J Biol Chem* 2013;288:15085–15097.

44 Liu K, Lin B, Zhao M et al. The multiple roles for Sox2 in stem cell maintenance and tumorigenesis. *Cell Signal* 2013;25:1264–1271.

45 Wegner M. SOX after SOX: SOXession regulates neurogenesis. *Genes Dev* 2011;25:2423–2428.

46 Keramari M, Razavi J, Ingman KA et al. Sox2 is essential for formation of trophectoderm in the preimplantation embryo. *PLoS ONE* 2010;5:e13952.

47 Mauksch C, Jones KS, Connor B. Concise review: The involvement of SOX2 in direct reprogramming of induced neural stem/precursor

cells. *STEM CELLS TRANSLATIONAL MEDICINE* 2013; 2:579–583.

48 Liu Y, Zheng B, Zhang XH et al. Localization and function of KLF4 in cytoplasm of vascular smooth muscle cell. *Biochem Biophys Res Commun* 2013;436:162–168.

49 Liu Z, Yang H, Luo W et al. Loss of cytoplasmic KLF4 expression is correlated with the progression and poor prognosis of nasopharyngeal carcinoma. *Histopathology* 2013;63:362–370.

50 Ezeh UI, Turek PJ, Reijo RA et al. Human embryonic stem cell genes OCT4, NANOG, STELLAR, and GDF3 are expressed in both seminoma and breast carcinoma. *Cancer* 2005; 104:2255–2265.

51 Wen J, Park JY, Park KH et al. Oct4 and Nanog expression is associated with early stages of pancreatic carcinogenesis. *Pancreas* 2010;39:622–626.

52 Zhang S, Balch C, Chan MW et al. Identification and characterization of ovarian cancer-initiating cells from primary human tumors. *Cancer Res* 2008;68:4311–4320.

53 Gu TT, Liu SY, Zheng PS. Cytoplasmic NANOG-positive stromal cells promote human cervical cancer progression. *Am J Pathol* 2012; 181:652–661.

54 Cho J, Chang H, Kwon SC et al. LIN28A is a suppressor of ER-associated translation in embryonic stem cells. *Cell* 2012;151:765–777.

55 Moss EG, Tang L. Conservation of the heterochronic regulator Lin-28, its developmental expression and microRNA complementary sites. *Dev Biol* 2003;258:432–442.

56 Qiu C, Ma Y, Wang J et al. Lin28-mediated post-transcriptional regulation of Oct4 expression in human embryonic stem cells. *Nucleic Acids Res* 2010;38:1240–1248.

57 Craig RW, Buchan HL, Civin CI et al. Altered cytoplasmic/nuclear distribution of the c-myc protein in differentiating ML-1 human myeloid leukemia cells. *Cell Growth Differ* 1993;4:349–357.

58 Hann SR, Eisenman RN. Proteins encoded by the human c-myc oncogene: Differential expression in neoplastic cells. *Mol Cell Biol* 1984;4: 2486–2497.

59 Dueck AC, Reinholz MM, Geiger XJ et al. Impact of c-MYC protein expression on outcome of patients with early-stage HER2+ breast cancer treated with adjuvant trastuzumab NCCCTG (Alliance) N9831. *Clin Cancer Res* 2013;19: 5798–5807.

60 Di J, Duiveman-de Boer T, Zusterzeel PL et al. The stem cell markers Oct4A, Nanog and c-Myc are expressed in ascites cells and tumor tissue of ovarian cancer patients. *Cell Oncol (Dordr)* 2013;36:363–374.

61 Spitzbarth I, Baumgärtner W, Beineke A. The role of pro- and anti-inflammatory cytokines in the pathogenesis of spontaneous canine CNS diseases. *Vet Immunol Immunopathol* 2012;147: 6–24.

62 Profyris C, Cheema SS, Zang D et al. Degenerative and regenerative mechanisms governing spinal cord injury. *Neurobiol Dis* 2004; 15:415–436.

63 Spitzbarth I, Bock P, Haist V et al. Prominent microglial activation in the early proinflammatory immune response in naturally occurring canine spinal cord injury. *J Neuropathol Exp Neurol* 2011;70:703–714.

64 Lee JH, Chung WH, Kang EH et al. Schwann cell-like remyelination following transplantation of human umbilical cord blood (hUCB)-derived mesenchymal stem cells in dogs with acute spinal cord injury. *J Neurol Sci* 2011;300: 86–96.

65 Ryu HH, Kang BJ, Park SS et al. Comparison of mesenchymal stem cells derived from fat, bone marrow, Wharton’s jelly, and umbilical cord blood for treating spinal cord injuries in dogs. *J Vet Med Sci* 2012;74:1617–1630.

66 Ryu HH, Lim JH, Byeon YE et al. Functional recovery and neural differentiation after transplantation of allogenic adipose-derived stem cells in a canine model of acute spinal cord injury. *J Vet Sci* 2009;10:273–284.

67 Lim JH, Byeon YE, Ryu HH et al. Transplantation of canine umbilical cord blood-derived mesenchymal stem cells in experimentally induced spinal cord injured dogs. *J Vet Sci* 2007; 8:275–282.

68 Park SS, Lee YJ, Lee SH et al. Functional recovery after spinal cord injury in dogs treated with a combination of Matrigel and neural-induced adipose-derived mesenchymal stem cells. *Cytotherapy* 2012;14:584–597.

69 Park SS, Byeon YE, Ryu HH et al. Comparison of canine umbilical cord blood-derived mesenchymal stem cell transplantation times: Involvement of astrogliosis, inflammation, intracellular actin cytoskeleton pathways, and neurotrophin-3. *Cell Transplant* 2011;20: 1867–1880.

70 Kim BG, Kang YM, Phi JH et al. Implantation of polymer scaffolds seeded with neural stem cells in a canine spinal cord injury model. *Cytotherapy* 2010;12:841–845.

71 Lee SH, Chung YN, Kim YH et al. Effects of human neural stem cell transplantation in canine spinal cord hemisection. *Neurol Res* 2009;31: 996–1002.

72 Lee JH, Chang HS, Kang EH et al. Percutaneous transplantation of human umbilical cord blood-derived multipotent stem cells in a canine model of spinal cord injury. *J Neurosurg Spine* 2009;11:749–757.

73 Jung DI, Ha J, Kang BT et al. A comparison of autologous and allogenic bone marrow-derived mesenchymal stem cell transplantation in canine spinal cord injury. *J Neurol Sci* 2009; 285:67–77.

74 Jeffery ND, Lakatos A, Franklin RJ. Autologous olfactory glial cell transplantation is reliable and safe in naturally occurring canine spinal cord injury. *J Neurotrauma* 2005;22: 1282–1293.

75 Al-Nbaheen M, Vishnubalaji R, Ali D et al. Human stromal (mesenchymal) stem cells from bone marrow, adipose tissue and skin exhibit differences in molecular phenotype and differentiation potential. *Stem Cell Rev* 2013;9: 32–43.



See www.StemCellsTM.com for supporting information available online.